Chemical modifications of imidazole-containing alkoxyamines increase C-ON bond homolysis rate: Effects on their cytotoxic properties in glioblastoma cells

Duje Buric, Christine Chacon, Gerard Audran, Diane Braguer, Sylvain R.A. Marque, Manon Carre, Paul Bremond, Toshihide Yamasaki

Chemical modifications of imidazole-containing alkoxyamines increase C–ON bond homolysis rate: effects on their cytotoxic properties in glioblastoma cells

Toshihide Yamasaki [a, #], Duje Buric [b, #], Christine Chacon [b], Gérard Audran [a], Diane Braguer [c,d], Sylvain R. A. Marque [a, e], Manon Carré [b, *], Paul Brémond [a,b, *]

[a] *Aix Marseille Univ, CNRS, ICR, Marseille, France*

[b] *Aix Marseille Univ, CNRS, INSERM, Institut Paoli-Calmettes, CRCM, Marseille, France*

[c] *Aix Marseille Univ, CNRS, INP, Marseille, France*

[d] *Aix Marseille Univ, APHM, Hôpital Timone, Marseille, France*

[e] *N.N. Vorozhtsov Novosibirsk Institute of Organic Chemistry, Lavrentieva 9, Novosibirsk 630090, Russian Federation*

[#] These authors contributed equally.

* corresponding authors

E-mail addresses: *manon.carre@univ-amu.fr , paul.bremond@univ-amu.fr*

Abstract:

Previously, we described alkoxyamines bearing a pyridine ring as new pro-drugs with low molecular weights and theranostic activity. Upon chemical stimulus, alkoxyamines undergo homolysis and release free radicals, which can, reportedly, enhance magnetic resonance imaging and trigger cancer cell death. In the present study, we describe the synthesis and the anti-cancer activity of sixteen novel alkoxyamines that contain an imidazole ring. Activation of the homolysis was conducted by protonation and/or methylation. These new molecules displayed cytotoxic activities towards human glioblastoma cell lines, including the U251-MG cells that are highly resistant to the conventional chemotherapeutic agent Temozolomide. We further showed that the biological activities of the alkoxyamines were not only related to their half-life times of homolysis. We lastly identified the alkoxyamine *(RS/SR)*-**4a**, with both a high antitumor activity and favorable $\log D_{7.4}$ and pK_a values, which make it a robust candidate for blood-brain barrier penetrating therapeutics against brain neoplasia.

Keywords:

Alkoxyamines, Alkyl radicals, Glioblastoma, Antitumor activity.

1. Introduction

The blood-brain barrier (BBB) is a semipermeable membrane barrier indispensable for the normal function of the central nervous system (CNS). Not only it hinders influx of most compounds and microbes from blood to brain but also it blocks most of therapeutics from reaching their targets in the brain. As a consequence, very few chemotherapeutic agents are available for treatment of brain tumors, such as glioblastoma, which are among the most aggressive and common brain tumor in adults as well as children. In the absence of active transport through the BBB, the molecular weight (MW), lipophilicity (logP), distribution coefficient (logD), hydrogen bond donors (HBD) and ionization of compound (pK_a) are among the most important factors for the diffusion of the therapeutic agents [1]. Therefore, novel low-MW molecules active against cancer cells are exceptionally interesting in the field of cancer therapeutics since they are more prone to penetrate BBB and thus might be used against glioblastoma.

Alkoxyamines, with R^1–ONR^2R^3 general structure, are compounds able to undergo homolysis of the labile C–ON bond to release a transient alkyl radical (R^1•) and a generally stable nitroxide (R^2R^3NO•) [2-4]. The main application of these compounds is the nitroxide-mediated controlled radical polymerization [5]. Interestingly, we recently proposed a new application of these low-molecular weight compounds as theranostic agents, *i.e.* with both therapeutic and diagnostic roles in fighting malignant tumors [6]. Indeed, we demonstrated that the released nitroxide from a pyridine-containing alkoxyamine can be used to perform imaging by the Overhauser-enhanced MRI (OMRI) technique, while the released alkyl radical triggered the apoptosis of cancer cells *in vitro* (Scheme 1) [7].

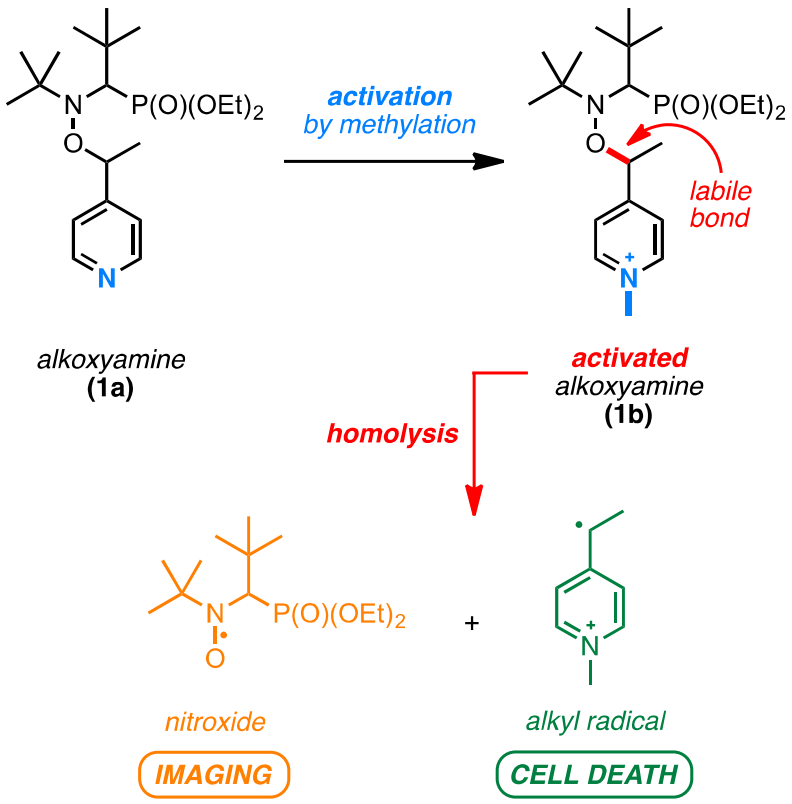

Scheme 1 Alkoxyamines as theranostic agents

However, the low pK_a of the pyridine ring of alkoxyamine **1a** (pK_a = 4.70) was an unfavorable aspect since it precludes the protonation of the ring in physiological conditions, *i.e.* at pH 7.4, and it required a beforehand activation by methylation to obtain the labile alkoxyamine **1b** ($t_{1/2}$ = 45 min) [8]. Furthermore, **1b** showed moderate cytotoxicity against glioblastoma cell lines. Therefore, these results prompted us to replace the pyridine ring of **1a** by an imidazole ring (pK_a = 6.95), a moiety that is widely considered as biocompatible and is present in many natural compounds and drugs [9]. Herein, we report the synthesis of sixteen new alkoxyamines that contain an imidazole ring grafted at the *C-2* (**2a-c**), *N-1* (**3a-b**) or *C-4* (**4a-c**) positions, respectively, and in this study, we will determine their kinetic properties and assess their therapeutic potential for glioblastoma (Figure 1). All these alkoxyamines are based on the same nitroxide part as **1b**, *i.e.* **SG1** nitroxide, as it affords labile alkoxyamines and as its imaging properties were already highlighted [7].

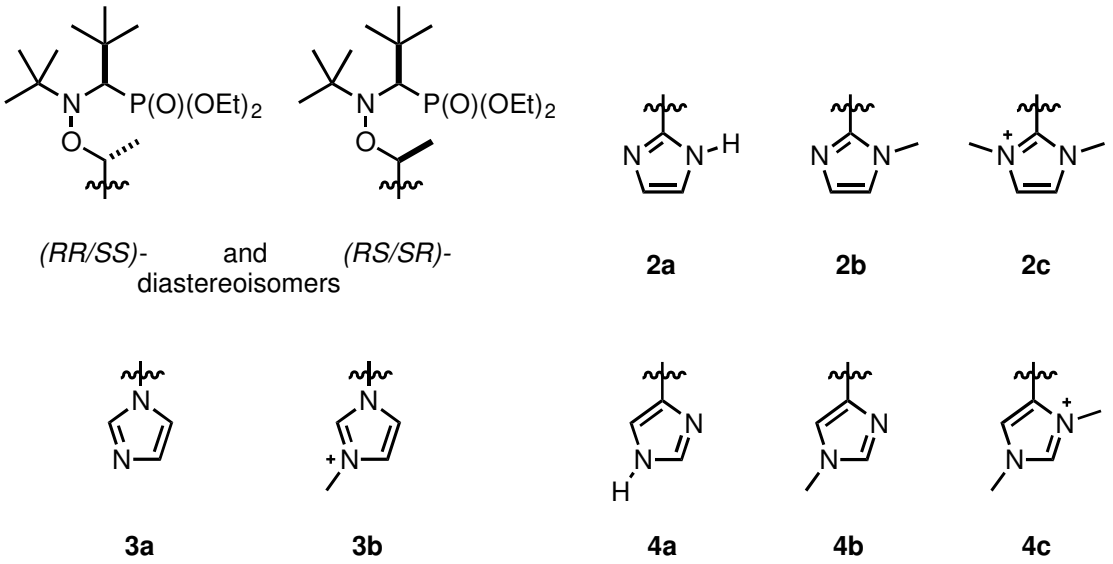

Figure 1 Structures of the alkoxyamines synthesized and evaluated in this work

2. Results and discussion

2.1. Synthesis of new alkoxyamines containing an imidazole ring

Synthesis of an alkoxyamine generally requires the *in-situ* generation of an alkyl radical followed by nitroxide-trapping of the latter. One of the most convenient methods for this purpose is the combination of an activated double bond and a particular catalytic system, based on a manganese-salen complex, with $NaBH_4$ in *i*-PrOH and under air atmosphere. Therefore, Mn-catalyzed coupling of **SG1** nitroxide (*N*-(2-methylpropyl)-*N*-(1-diethylphosphono-2,2-dimethylpropyl)-*N*-oxyl) and 2-vinyl-1*H*-imidazole gave alkoxyamine **2a** in 54% yield and as two diastereoisomers, which were purified and separated by column chromatography to give *(RR/SS)*-**2a** and *(RS/SR)*-**2a** (Scheme 2). The same procedure was repeated to obtain alkoxyamines **3a** (37% yield) and **4a** (39% yield) from 1-vinyl-1*H*-imidazole and 4-vinyl-1*H*-imidazole, respectively, as well as mono-methylated analogue **2b** (54% yield) from 1-methyl-2-vinyl-1*H*-imidazole. Dimethylimidazolium analogue **2c** and monomethylimidazolium analogue **3b** were obtained by methylation of each diastereoisomer

of **2b** and **3a**, respectively, using methyl *p*-toluenesulfonate in THF. Finally, mono-methylated analogue **4b** and dimethylimidazolium analogue **4c** were both obtained directly by methylation of **4a** using methyl iodide and potassium carbonate in dichloromethane (see experimental section). All compounds were obtained as pure and diastereomerically homogeneous compounds and were characterized by NMR (^{1}H, ^{13}C, ^{31}P) and HRMS to ascertain their chemical structures. Their relative configurations were determined by single-crystal X-ray diffraction, as some compounds were isolated as crystals (see supplementary material) [10].

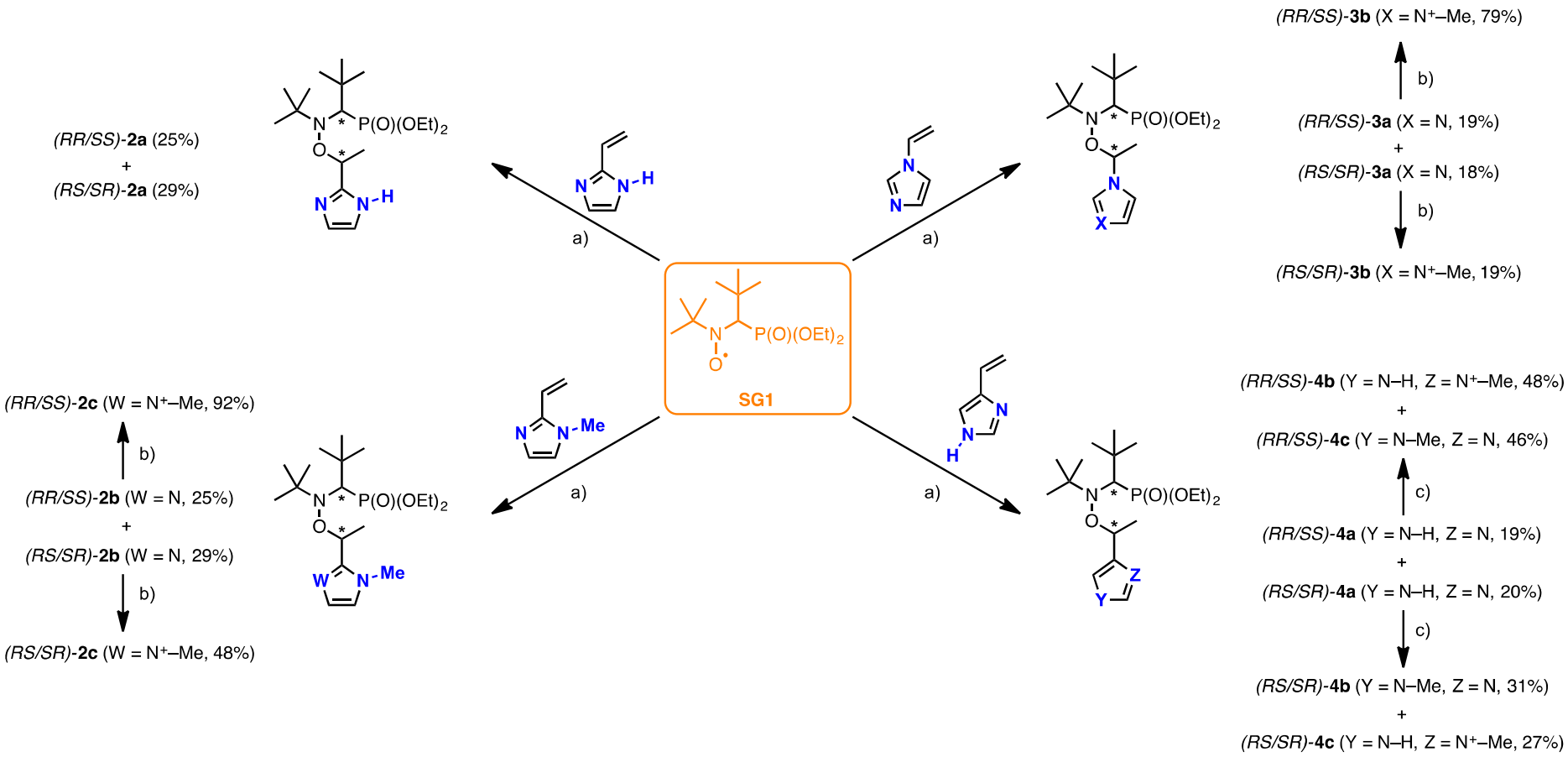

Scheme 2 Synthesis of alkoxyamines *(RR/SS)*- and *(RS/SR)*- **2a-c**, **3a-b**, **4a-c**: a) $MnCl_2$, *N*,*N'*-bis(salicylidene)ethylenediamine (salen), $NaBH_4$, *i*-PrOH, air; b) methyl *p*-toluenesulfonate, THF; c) MeI, K_2CO_3, CH_2Cl_2.

2.2. Kinetic investigations

The p*K*a values of alkoxyamines were determined by titration by ^{1}H NMR of signals of the aromatic moiety at various pH in D_2O/CD_3OD (1:1 *v/v*) [11]. All p*K*a were *ca.* 1-2 units higher than the previously investigated alkoxyamine **1a**, that contains a pyridine ring (Table 1).

Then, the stability of the new alkoxyamines was investigated by EPR in aqueous solutions, using oxygen as radical scavenger. Thermolysis experiments were performed at different pH, *i.e.* to obtain >99% of protonated or non-protonated forms of imidazole rings. Homolysis rates (k_d) were obtained and the corresponding activation energies (E_a) were calculated using Arrhenius equation and the averaged pre-exponential factor $A = 2.4.10^{14}$ s^{-1}. Half-life times ($t_{1/2}$) were also re-estimated at 37 °C to allow direct comparisons between compounds at physiological temperature. Depending on pH, clear differences in E_a and $t_{1/2}$ values were observed (Table 1 and supplementary material).

Table 1 pK_a, activation energies (E_a), and half-life time ($t_{1/2}$) at 37 °C for alkoxyamines *(RR/SS)*- and *(RS/SR)*-**2a-b**, **3a**, **4a-b** at different pH (see supplementary material for details).

Alkoxyamine	pK_a	conditions[a]	E_a (kJ/mol)[b]	$t_{1/2}$ (37 ºC)[c]	Alkoxyamine	pK_a	conditions[a]	E_a (kJ/mol)[b]	$t_{1/2}$ (37 ºC)[c]
(RR/SS)-**2a**	6.09	pH = 10.3	121.6	10 d	*(RS/SR)*-**2a**	6.04	pH = 10.3	122.3	13 d
		pH = 2.2	111.1	4 h			pH = 2.2	111.7	5 h
(RR/SS)-**2b**	6.28	pH = 10.3	120.0	130 h	*(RS/SR)*-**2b**	6.50	pH = 10.3	116.9	39 h
		pH = 2.2	109.7	144 min			pH = 2.2	109.2	119 min
(RR/SS)-**3a**	5.62	DMSO	148.9	> 1000 y	*(RS/SR)*-**3a**	5.81	DMSO	144.9	> 200 y
		DMSO + TsOH[d]	142.8	> 100 y			DMSO + TsOH[d]	140.9	> 50 y
(RR/SS)-**4a**	6.11	pH = 10.3	123.0	17 d	*(RS/SR)*-**4a**	6.13	pH = 10.3	123.3	19 d
		pH = 2.2	119.4	103 h			pH = 2.2	121.2	8 d
(RR/SS)-**4b**	6.76	pH = 10.3	126.4	65 d	*(RS/SR)*-**4b**	6.56	pH = 10.3	126.6	70 d
		pH = 2.2	118.2	65 h			pH = 2.2	120.5	7 d

[a] Solutions were buffered with $Na_2CO_3/NaHCO_3$ (pH = 10.3) or HCl/KCl (pH = 2.2). [b] Calculated with experimental k_d values using Arrhenius equation and $A = 2.4.10^{14}$ s^{-1}. [c] Calculated at 37 ºC using re-estimated k_d values. [d] TsOH = *para*-toluenesulfonic acid.

At basic pH, *(RR/SS)*-**2a** and *(RS/SR)*-**2a**, as well as *(RR/SS)*-**4a** and *(RS/SR)*-**4a**, exhibited E_a values similar to other SG1-based alkoxyamines bearing a secondary benzylic-type alkyl radical. Small differences of 0.3-0.7 kJ/mol were observed between diastereoisomers within the conventional ranges, as already documented [12]. From these E_a, $t_{1/2}$ of 10-19 d at 37 ºC were calculated. However, *(RR/SS)*- and *(RS/SR)*-**3a** were found to be very stable in aqueous solutions. Therefore, DMSO was used as solvent in order to reach higher temperature and accelerate thermolysis experiments. Very high E_a were determined and, consequently, estimated $t_{1/2}$ at 37 ºC clearly illustrated the high stability of alkoxyamine **3a**. The differences of stability between the alkoxyamines were explained by performing calculations of the radical stabilization energy (RSE) of benzylic radical models. Indeed, the RSE of the calculated radicals were –3.6 kJ/mol for the series **2** and +4.3 kJ/mol for the series **4** (see supplementary material). These values indicated that the stabilization of the odd electron is better in the series **2** than in the series **4**, thus confirming the observed reactivity. On the other hand, in the case of the series **3**, the calculated RSE was highly positive (+20.4 kJ/mol), *i.e.* small or no delocalization of the odd electron, thus confirming the exceptional stability for this SG1-based alkoxyamine [13].

At acidic pH, as expected, acceleration of the homolysis rate by protonation of the imidazole ring was observed for *(RR/SS)*-**2a** and *(RS/SR)*-**2a**, as well as *(RR/SS)*-**4a** and *(RS/SR)*-**4a**. However, the efficiency of the proton-triggered activation strongly depends on the position of the nitrogen atoms in the imidazole ring. Indeed, we observed decreases in E_a of *ca.* 10.5 kJ/mol for *(RR/SS)*-**2a** and *(RS/SR)*-**2a**, while it was only *ca.* 2-4 kJ/mol for *(RR/SS)*-**4a** and *(RS/SR)*-**4a**. For **3a**, upon protonation with PTSA in DMSO, activation was also observed, as E_a of *(RR/SS)*-**3a** decreased of 6.1 kJ/mol, while it decreased of 4.0 kJ/mol for *(RS/SR)*-**3a**.

Such differences in reactivity depending on the position of the nitrogen atoms were already observed by us on pyridine-containing alkoxyamines **1a** and other analogues [14]. Indeed,

while the development of the positive charge due to protonation affects the entire heteroaromatic ring, thus increasing its polar effect, it is however more prevailing on particular positions of the imidazolium ring, *i.e. N*-1, *C*-2 and *N*-3 positions (Scheme 3). Hence, in the series **2**, a positive charge can be developed on the aromatic carbon atom in α-position of the labile bond (*i.e. C-2* position), thus strong chemical activation of the homolysis, *i.e.* acceleration of 60-times, can be achieved. On the other hand, in the series **4**, the positive charge cannot be developed in the adequate position to obtain chemical activation, which would be the *C-4* position, thus only the increase of the polarity, due to the protonation of the heteroaromatic moiety, is probably the sole responsible for the activation, with only a small effect (*ca.* 2-4-times acceleration). In the series **3**, despite the apparent favorable development of the positive charge in the adequate position (i.e. *N-1* position), the strong destabilization of the released radical leads to a high stability of the corresponding alkoxyamines (*vide supra*) [15].

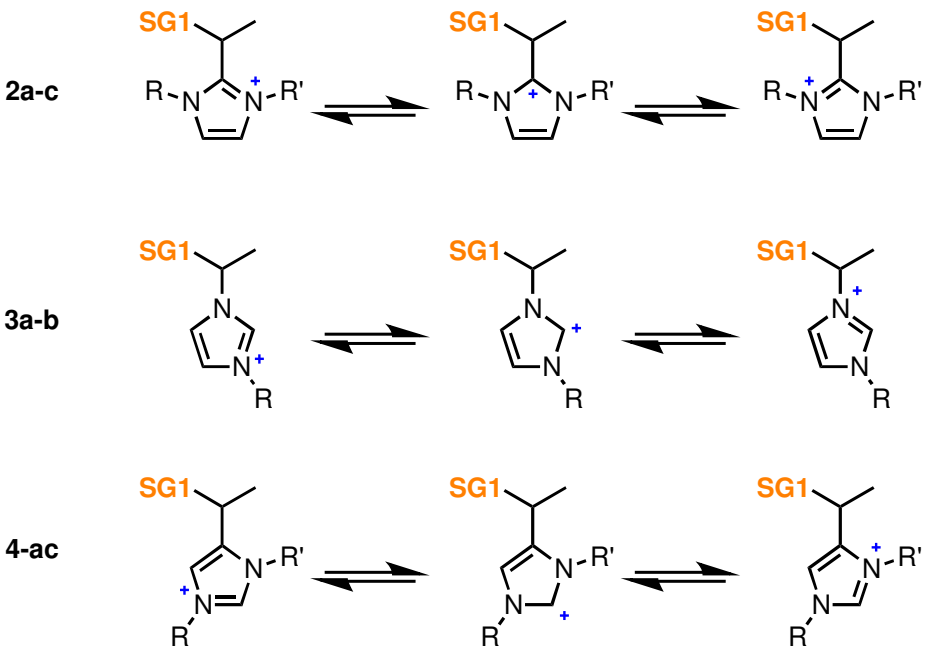

Scheme 3 Mesomeric forms of alkoxyamines (R, R' = H or Me)

Monomethylation of **2a** into **2b** afforded a loss of 1.6 to 5.4 kJ/mol at basic pH depending on the diastereoisomers, *i.e.* acceleration of homolysis of 2- to 8-times. After protonation, an additional decrease of 7.7 to 10.3 kJ/mol, *i.e.* acceleration of 20 to 50-times, was observed. Thus, by combining methylation and protonation, the total decrease was *ca.* 12-13 kJ/mol, meaning *ca.* 100- to 150-times acceleration of homolysis rate. This increased activation can be ascribed to an increase of the steric hindrance of the alkyl part, leading to an acceleration of the homolysis rate. However, methylation of **4a** into **4b** was less striking, leading to an overall decrease of *ca*. 3-5 kJ/mol. *i.e.* only *ca.* 3- to 6-times acceleration, probably because the increase of the steric hindrance due to the methylation is farther away from the reactive center and therefore its effect is negligible.

In order to grasp their potential reactivity in biological conditions, kinetics of all these alkoxyamines were also measured at pH 7.4 (Table 2). Due to its very high E_a, kinetic of alkoxyamine **3a** was not re-measured. However, intermediates values of E_a, as well as of $t_{1/2}$, were obtained, as pK_a values of these compounds are lower than 7.4, thus limiting the activation of the homolysis. Therefore, in order to circumvent this issue and to potentially achieve full activation at pH 7.4, we followed the same approach used for alkoxyamine **1a** by converting the imidazole ring into the corresponding imidazolium by methylation investigating dimethylimidazolium-alkoxyamines **2c**, **3b** and **4c** at pH 7.4. For alkoxyamine **2c**, overall decreases of 8.1 to 11.7 kJ/mol, *i.e.* acceleration of 24- to 90-times, were observed, thus confirming that it is unstable at pH 7.4. Similarly, for alkoxyamine **4c**, a decrease of E_a (*ca.* 7 kJ/mol) was observed, *i.e.* acceleration factor of *ca.* 15-times. However, for alkoxyamine **3b**, despite that decreases of *ca.* 10 to 14 kJ/mol were observed, half-life times were still very high.

Table 2 Activation energies (E_a) and half-life time ($t_{1/2}$) at 37 °C for alkoxyamines *(RR/SS)*- and *(RS/SR)*-**2a-c**, **3a-b**, **4a-c** at pH = 7.4 (see supplementary material for details).

Alkoxyamine	conditions[a]	E_a (kJ/mol)[b]	$t_{1/2}$ (37 °C)[c]	Alkoxyamine	conditions[a]	E_a (kJ/mol)[b]	$t_{1/2}$ (37 °C)[c]
(RR/SS)-**2a**	pH = 7.4	118.0	60 h	*(RS/SR)*-**2a**	pH = 7.4	118.8	81 h
(RR/SS)-**2b**	pH = 7.4	116.3	31 h	*(RS/SR)*-**2b**	pH = 7.4	113.5	10 h
(RR/SS)-**2c**	pH = 7.4	113.5	10 h	*(RS/SR)*-**2c**	pH = 7.4	110.6	204 min
(RR/SS)-**3a**	pH = 7.4	-[d]	-[d]	*(RS/SR)*-**3a**	pH = 7.4	-[d]	-[d]
(RR/SS)-**3b**	pH = 7.4	135.2	5 y	*(RS/SR)*-**3b**	pH = 7.4	135.2	5 y
(RR/SS)-**4a**	pH = 7.4	122.1	12 d	*(RS/SR)*-**4a**	pH = 7.4	122.3	13 d
(RR/SS)-**4b**	pH = 7.4	124.7	33 d	*(RS/SR)*-**4b**	pH = 7.4	123.6	22 d
(RR/SS)-**4c**	pH = 7.4	115.8	25 h	*(RS/SR)*-**4c**	pH = 7.4	116.1	29 h

[a] Solutions were buffered with HEPES/NaOH buffer (50 mM, pH = 7.4) with 0.15 mM of NaCl.

[b] Calculated with experimental k_d values using Arrhenius equation and $A = 2.4.10^{14}$ s^{-1}.

[c] Calculated at 37 °C using re-estimated k_d values.

[d] Not determined (see text).

2.3. Cytotoxic properties of the alkoxyamines

We previously reported that alkoxyamines display lethal properties in glioblastoma cells, but with a poor level of efficacy [7]. Therefore, we investigated whether the cytotoxicity of the new unstable alkoxyamines (**2a-c** and **4a-c**) was improved in human glioblastoma cell lines and whether stable alkoxyamines (**3a-b**) stay inert due to their extremely long half-life. The cytotoxic potential of the sixteen novel alkoxyamines (**2a-c**, **3a-b** and **4a-c**) was first evaluated in the human U87-MG cell line, derived from malignant glioma that we previously used for research of new active compounds in glioblastomas [16-19]. All alkoxyamines exerted a dose-dependent inhibition of the cancer cell survival after a 72 h-treatment (Figure

2a and b). IC_{50} values, *i.e.* concentrations that half-reduced U87-MG cell survival, ranged from 25 to 380 µM (Figure 2c). Among the twelve unstable alkoxyamines (**2a-c** and **4a-c**) evaluated in the present study, eight were more effective in reducing cancer cell survival than the previously investigated alkoxyamine **1b**, whose IC_{50} value reached 250 µM in similar experimental conditions [7]. It is especially notable with the compound *(RS/SR)*-**4a**, which displayed the highest efficacy and was 10 times more active than **1b** in the same U87-MG cell model (Figure 2b and c). The promising anticancer property of this novel alkoxyamine was confirmed by light-microscopy, with a significant decrease in cell density as compared with the other molecules (Figure 2d).

Among the four stable alkoxyamines (**3a-b**), three of them exerted a significant cytotoxicity with IC_{50} ranging from 101 to 166 µM, suggesting that either they release alkyl radicals by an alternative mechanism or they are toxic without undergoing homolysis. Therefore, in order to explore whether the novel alkoxyamines – both stable and unstable – exert their cytotoxicity through the release of alkyl radical, we co-treated U87-MG cells with IC_{50} concentration of both alkoxyamines and the alkyl radical scavenger Troxerutin [6]. The experiment showed that cytotoxicity of all the twelve unstable alkoxyamines (**2a-c** and **4a-c**) was significantly inhibited by Troxerutin confirming that their efficacy comes from the release of alkyl radical (Figure 2d). However, cytotoxicity of the four stable alkoxyamines (**3a-b**) remained intact despite the presence of the alkyl radical scavenger (Figure 2d). Their mechanism of action is thus independent of homolysis and will undergo further analysis.

Furthermore, cytotoxicity of the twelve unstable alkoxyamines (**2a-c** and **4a-c**) emerges faster than the chemical half-life should have suggested. Chemical half-life of the alkoxyamines in our study was measured *in vitro* in aqueous solution, which provides anisotropic conditions that are not present in heterogeneous cell culture medium or within the cytoplasm. Alkoxyamines are likely to obtain other conformations that increase homolysis rate due to

biological environment: *e.g.* various proteins alkoxyamines may be complexed to, biological membranes they may be inserted in, or viscous intracellular cytosol that may result in conformational changes. Details of the mechanism of activation *in cellulo* are under investigation and will be addressed in the follow-up of the project.

A common feature of the unstable alkoxyamines (**2a-c** and **4a-c**) is that the charged molecules were less cytotoxic towards cancer cells than the neutral ones. To mention but a few examples, the monomethylimidazole alkoxyamines *(RR/SS)*-**4b** and *(RS/SR)*-**4b** were 4.4 and 4.9 times more active than the dimethylimidazolium alkoxyamines *(RR/SS)*-**4c** and *(RS/SR)*-**4c**, respectively. Indeed, it is generally accepted that neutral compounds are more readily able to cross non-polar lipid bilayers, unlike charged compounds where this process is energetically disfavored [20]. Thus, despite the fact that the dimethylimidazolium alkoxyamines have lower $t_{1/2}$, *i.e.* undergo faster homolysis, the charged heteroaromatic ring may disturb the targeting of the molecules to cell plasma membrane and/or to intracellular compartments.

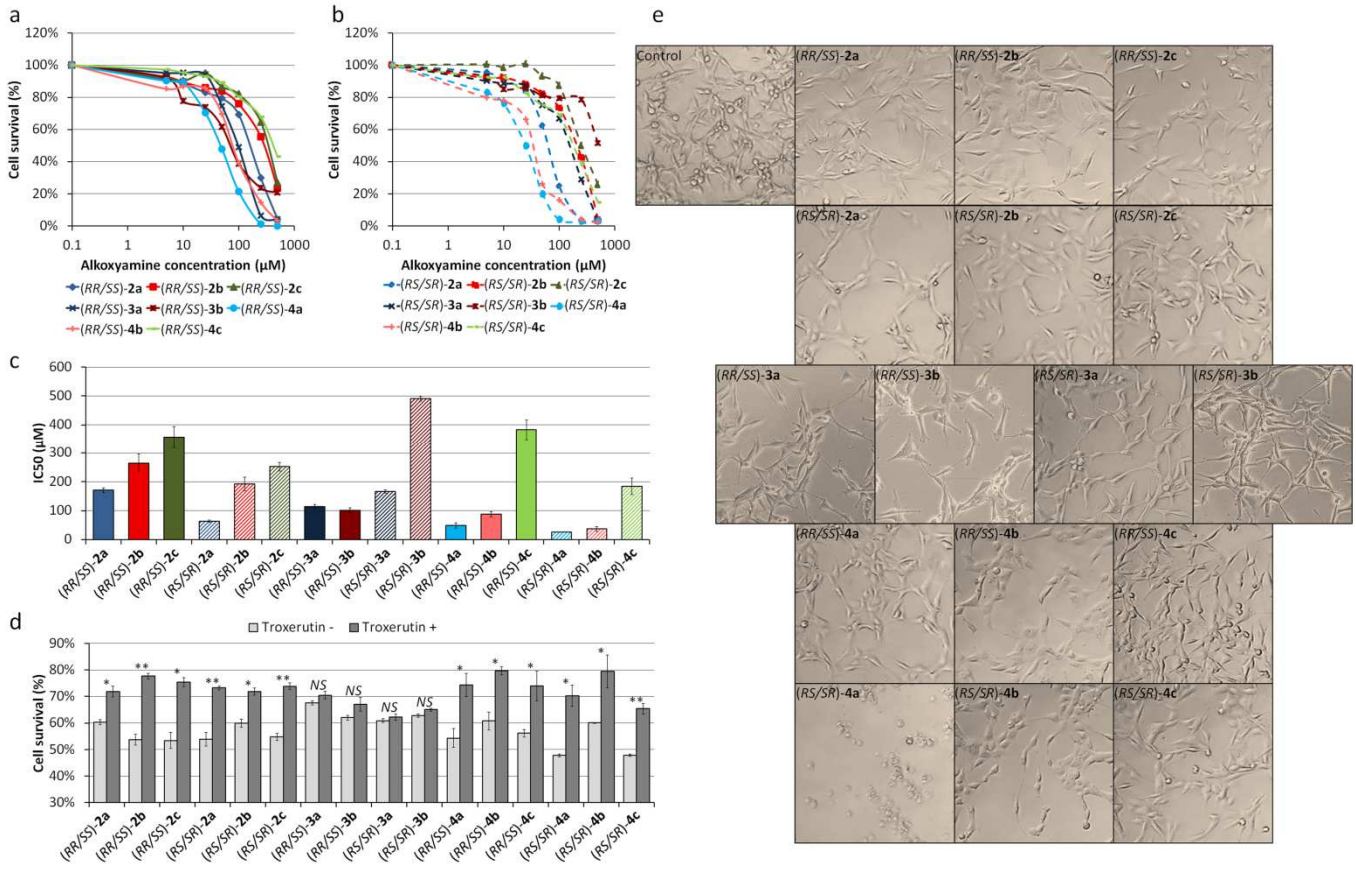

Figure 2 Cytotoxicity of alkoxyamines **2a-c, 3a-b** and **4a-c** towards U87-MG human glioblastoma cell line, after a 72 h-treatment. (a) Cell survival measured by MTT-assay of (*RR/SS*)-**2a-c, 3a-b** and **4a-c** in 2D-culture of U87-MG cell line; (b) Cell survival measured by MTT-assay of (*RS/SR*)-**2a-c, 3a-b** and **4a-c** in 2D-culture of U87-MG cell line; (c) IC_{50} measured by MTT-assay of (*RR/SS*)- and (*RS/SR*)-**2a-c, 3a-b** and **4a-c** in U87-MG cell line; (d) Cell survival of U87-MG measured by MTT-assay of IC_{50} concentrations of (*RR/SS*)- and (*RS/SR*)-**2a-c, 3a-b** and **4a-c** in presence of equal concentrations of alkyl scavenger Troxerutin. * $p<0.05$ and ** $p<0.01$: significant variations between alkoxyamine alone *versus* its combination with Troxerutin, NS: non-significant variations (e) Representative pictures of U87-MG culture with each alkoxyamine at 50 µM.

Molecular weight (MW) and distribution coefficient (logD) value have been found to be the most discriminating factors in determining the permeability of drug candidates. For cases

where a drug reaches its target locations by passive mechanisms, the ideal logD has been defined to be up to 4 [21], and either >1.3 for compounds with molecular weight below 414 $g.mol^{-1}$ or >2.4 for higher molecular weights [22]. We therefore turned our attention to the *n*-octanol/PBS partition coefficient of the different alkoxyamines at physiological pH. As shown in Table 3, the $logD_{7.4}$ values measured for alkoxyamines **2c**, **3b** and **4c** confirmed that these molecules were not in the optimum range for biological activity. On the other hand, the molecular weights and $logD_{7.4}$ values of alkoxyamines **2a-b**, **3a** and **4a-b** make them more likely to enter the cells, in agreement with the U87-MG cell survival data.

Table 3 Molecular weight and measured *n*-octanol/PBS partition coefficient ($logD_{7.4}$) of alkoxyamines **2a-c**, **3a-b** and **4a-c**.

Alkoxyamine	Molecular weight ($g.mol^{-1}$)	$logD_{7.4}$	Alkoxyamine	Molecular weight ($g.mol^{-1}$)	$logD_{7.4}$
(RR/SS)-**2a**	389.5	3.6	*(RS/SR)*-**2a**	389.5	4.1
(RR/SS)-**2b**	403.5	3.4	*(RS/SR)*-**2b**	403.5	3.7
(RR/SS)-**2c**	418.5	-0.2	*(RS/SR)*-**2c**	418.5	0.5
(RR/SS)-**3a**	389.5	3.4	*(RS/SR)*-**3a**	389.5	3.4
(RR/SS)-**3b**	404.5	-0.1	*(RS/SR)*-**3b**	404.5	0.3
(RR/SS)-**4a**	389.5	3.7	*(RS/SR)*-**4a**	389.5	4.0
(RR/SS)-**4b**	403.5	3.5	*(RS/SR)*-**4b**	403.5	3.8
(RR/SS)-**4c**	418.5	0.8	*(RS/SR)*-**4c**	418.5	0.4

Furthermore, the results obtained in U87-MG cells were additionally validated in the human malignant astrocytoma U251-MG cells. We confirmed that all sixteen alkoxyamines reduced survival of glioblastoma cells in a dose-dependent manner and that the neutral molecules were more active than the charged ones (Figure 3a and b). Importantly, U251-MG cells do not respond to Temozolomide (IC_{50} TMZ = 455 µM; data not shown), the standard chemotherapy treatment for glioblastoma, pointing out the fact that alkoxyamines may circumvent drug

resistance in these refractory cancer cells. Compared with U87-MG cells, U251-MG cells were even more sensitive to alkoxyamines, as shown by the increase in *(RR/SS)*-**2a** and *(RS/SR)*-**2a** cytotoxicity by 38% and 36%, respectively (Figure 3c *versus* Figure 2c). The same applies to *(RS/SR)*-**4a**, which was again the most active alkoxyamine evaluated, with an IC_{50} value reduced to 20 µM (Figure 3c). Higher efficacy in U251-MG cells might be linked to their glycolytic phenotype that, by releasing a greater amount of lactic acid, may result in a faster acidification of the cell microenvironment [23]. In support to this, we measured the extracellular pH and showed that it remained at 7.5 in the medium sampled from the 48 h-cultures of U87-MG cells while it was reduced to 6.8 in U251-MG cell cultures (data not shown). This acidic cell microenvironment may then promote the homolysis of the prodrugs at a faster rate (Tables 1 and 2), and faster enough to observe increased cytotoxicities.

Stable alkoxyamines (**3a-b**) were again more cytotoxic than expected and their efficacy remained intact upon the combined treatment with the alkyl scavenger Troxerutin confirming that, also in U251-MG cells, toxicity of the alkoxyamines **3a-b** does not originate from homolysis and alkyl radical release (Figure 3d).

A crucial aspect of glioblastoma treatment concerns the ability of drugs to penetrate the BBB. This obstacle to drugs entering the CNS results from the tight junctions between the epithelial cells of the BBB and from the efflux pumps residing on astrocyte membranes of the BBB that counteract drug entry. In close relation to the parameters described above for cancer cell membranes permeability, permeability in brain capillaries has been related to drug lipophilicity, and hence to partition coefficient [1]. For the design of compounds where CNS penetration is required, $logD_{7.4}$ values were indeed given an optimal range between 2.0 and 4.0 [24], which is the case for the neutral alkoxyamines **2a** and **4a** (Table 3). The ability of these pro-drugs to be brain-penetrating drugs is also supported by the pK_a values, from 6.04 to 6.76 (Table 1), since compounds with pK_a above 5.5 have been identified as more likely to be

CNS-penetrant [25]. Lastly, glioblastoma drug candidates should not be substrates for efflux transporters, such as the P-glycoprotein (P-gp). Considering this active efflux, it has been proposed that compounds are likely to be non-substrates if they have accessible H-accepting atoms ≤ 4, molecular weight < 400 and a pK_a < 8 [26]. Thus, it can be assumed that the active efflux of the alkoxyamines **2a-b** and **4a-b** from the CNS may be minimized.

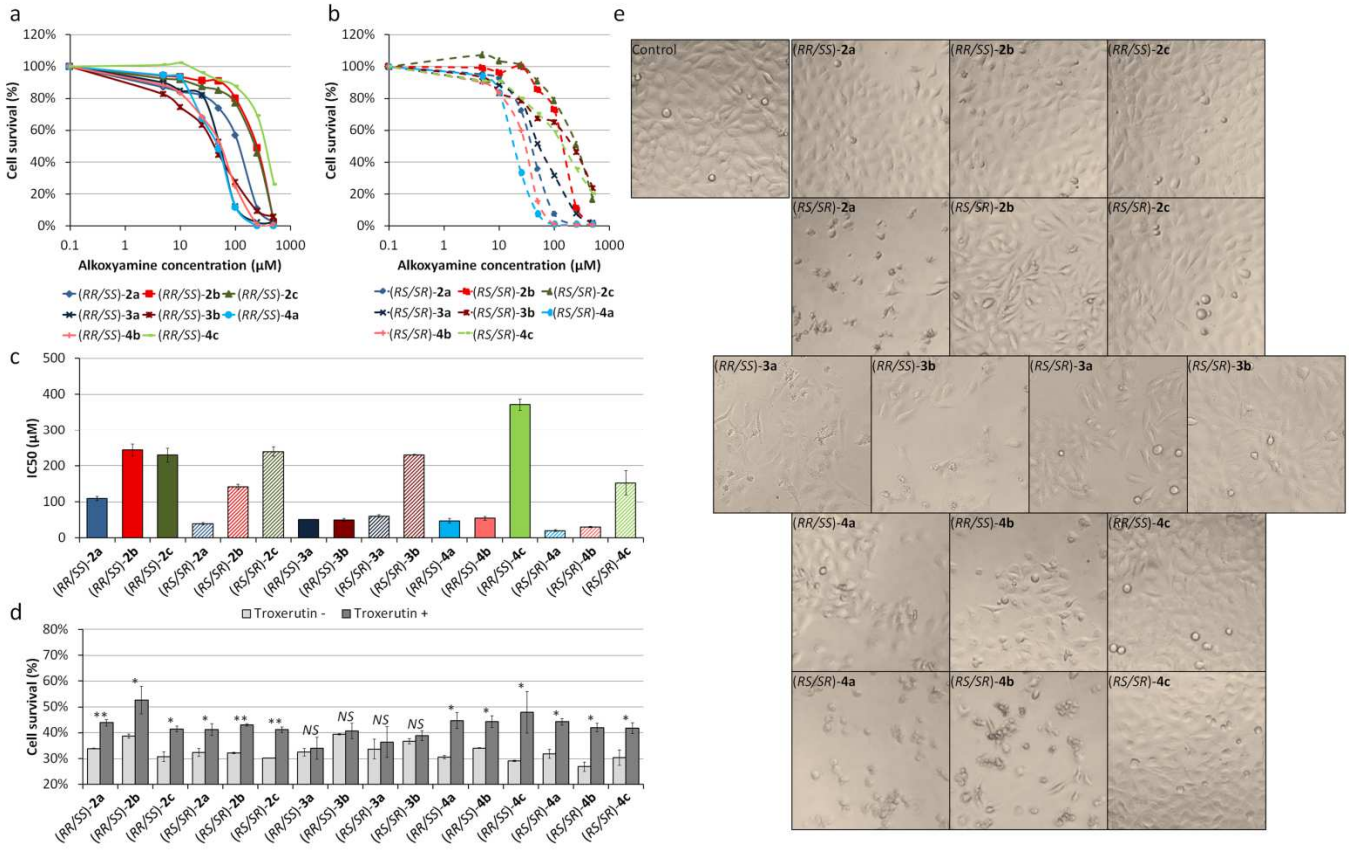

Figure 3 Cytotoxicity of alkoxyamines **2a-c, 3a-b** and **4a-c** towards U251-MG human glioblastoma cell line after a 72 h-treatment. (a) Cell survival measured by MTT-assay of (*RR/SS*)-**2a-c, 3a-b** and **4a-c** in 2D-culture of U251-MG cell line; (b) Cell survival measured by MTT-assay of (*RS/SR*)-**2a-c, 3a-b** and **4a-c** in 2D-culture of U251-MG cell line; (c) IC_{50} measured by MTT-assay of (*RR/SS*)- and (*RS/SR*)-**2a-c, 3a-b** and **4a-c** in U251-MG cell line; (d) Cell survival of U251-MG measured by MTT-assay of IC_{50} concentrations of (*RR/SS*)- and

(*RS/SR*)-**2a-c, 3a-b** and **4a-c** in presence of equal concentrations of alkyl scavenger Troxerutin. * $p<0.05$ and ** $p<0.01$: significant variations between alkoxyamine alone *versus* its combination with Troxerutin, NS: non-significant variations (e) Representative pictures of U251-MG culture with each alkoxyamine at 50 µM.

3. Conclusions

Our interdisciplinary work led to the synthesis and characterization of novel imidazole ring-containing alkoxyamines, and to the analysis of their activity against human cancer cells related to release of free radicals. The understanding of the structure-activity relationship for the unstable alkoxyamines (**2a-c** and **4a-c)**, by protonation and/or methylation, highlighted that their biological activities do not only correlate with their half-life time of homolysis, but rather also result from a tight balance between pK_a, $logD_{7.4}$ and molecular weight. Among the set of new alkoxyamines, we identified *(RS/SR)*-**4a** as the compound with the highest antitumor activity, including towards glioblastoma cells that are resistant to conventional chemotherapy. Furthermore, its favorable $logD_{7.4}$ and pK_a values make it a robust candidate for blood-brain barrier penetrating therapeutics against brain neoplasia. Thus, our results open new opportunities for future works to optimize the alkoxyamines with increased pharmacological activity and likely as few side effects as possible.

4. Experimental

4.1. Syntheses

4.1.1. General methods

All solvents and reagents were used as received. Routine monitoring of reactions was performed using silica gel 60 F_{254} TLC plates; spots were visualized using UV light and phosphomolybdic acid solution in EtOH, followed by heating. Purifications by column

chromatography were performed with silica gel 60 (230–400 mesh). ^{1}H, ^{13}C, and ^{31}P NMR spectra were recorded in $CDCl_3$ or DMSO-d_6 on 300 or 400 MHz spectrometers. Chemical shifts (δ) in ppm are reported using residual non-deuterated solvents as internal reference for ^{1}H and ^{13}C-NMR spectra, or using an internal sealed capillary filled with 85% H_3PO_4 for ^{31}P-NMR spectra.

4.1.2. Diethyl (1-((1-(1*H*-imidazol-2-yl)ethoxy)(*tert*-butyl)amino)-2,2-dimethylpropyl)phosphonate ((*RR/SS*)-2a and (*RS/SR*)-2a). To a stirred solution of salen ligand (0.07 g, 0.25 mmol, 0.05 eq.) in *i*-PrOH (7 mL) was added $MnCl_2$ (0.03 g, 0.25 mmol, 0.05 eq.) in an opened flask. After stirring with air bubbling at rt for 10 min, a solution of SG1 nitroxide (1.47 g, 5.0 mmol, 1.0 eq.) and 2-vinyl-1*H*-imidazole [27] (0.57 g, 6 mmol, 1.2 eq.) in *i*-PrOH (10 mL) was added, followed by solid $NaBH_4$ (0.19 g, 5 mmol, 1.0 eq.) added in small portions below 25 ºC. The mixture was stirred at rt for 3 h, and then sat. $NaHCO_3$ and CH_2Cl_2 were added and extracted with CH_2Cl_2. The combined organic phase was washed with brine, dried with $MgSO_4$, and concentrated to afford a crude product as a 1.4: 1 mixture of diastereoisomers (^{31}P-NMR ratio). The crude was separated by flash column chromatography (CH_2Cl_2: MeOH = 97: 3) to afford (*RR/SS*)-**2a** (0.50 g, 25%) and (*RS/SR*)-**2a** (0.56 g, 29%). (*RR/SS*)-**2a**: pale yellow solid; m.p.: 110 ºC (decomp.); R_f = 0.21 (CH_2Cl_2: MeOH = 19: 1); ^{1}H-NMR ($CDCl_3$, 400 MHz): δ 1.13 (s, 9 H), 1.20 (t, *J* = 7.1 Hz, 3 H), 1.25 (s, 9 H), 1.35 (t, *J* = 7.1 Hz, 3 H), 1.76 (d, *J* = 6.7 Hz, 3 H), 3.36 (d, *J* = 26.5 Hz, 1 H), 3.76 - 3.88 (m, 1 H), 3.92 - 4.09 (m, 2 H), 4.09 - 4.23 (m, 2 H), 5.29 (q, *J* = 6.4 Hz, 1 H), 6.96 (s, 2 H), 11.94 (br. s, 1 H); $^{13}C\{^{1}H\}$-NMR ($CDCl_3$, 75 MHz): δ 16.0 (d, *J* = 7.2 Hz), 16.1 (d, *J* = 6.1 Hz), 21.1 (s), 27.7 (s), 30.2 (d, *J* = 6.1 Hz), 35.4 (d, *J* = 3.9 Hz), 59.7 (d, *J* = 7.7 Hz), 61.4 (d, *J* = 6.6 Hz), 62.4 (s), 69.4 (d, *J* = 138.6 Hz), 77.7 (s), 149.6 (s); $^{31}P\{^{1}H\}$-NMR ($CDCl_3$, 162 MHz): δ 27.40; HRMS (ESI-TOF) m/z: $[M+H]^+$ Calcd for $C_{18}H_{37}N_3O_4P$ 390.2516; Found 390.2517; (*RS/SR*)-**2a**: pale yellow oil. R_f = 0.30 (CH_2Cl_2: MeOH = 19: 1); ^{1}H-NMR

($CDCl_3$, 400 MHz): δ 1.04 (s, 9 H), 1.19 (s, 9 H), 1.26 (t, *J* = 7.1 Hz, 3 H), 1.34 (t, *J* = 7.1 Hz, 3 H), 1.65 (d, *J* = 6.7 Hz, 3 H), 3.43 (d, *J* = 28.0 Hz, 1 H), 3.90 (ddq, *J* = 10.4, 9.0, 7.1, 7.1, 7.1 Hz, 1 H), 3.96 - 4.06 (m, 1 H), 4.06 - 4.19 (m, 2 H), 5.19 (q, *J* = 6.7 Hz, 1 H), 6.97 (d, *J* = 5.6 Hz, 2 H), 12.23 (br. s, 1 H); $^{13}C\{^1H\}$-NMR ($CDCl_3$, 75 MHz): δ 15.8 (d, *J* = 6.6 Hz), 16.1 (d, *J* = 6.1 Hz), 19.1 (s), 27.7 (s), 30.0 (d, *J* = 6.1 Hz), 35.0 (d, *J* = 5.0 Hz), 59.3 (d, *J* = 7.7 Hz), 61.58 (s), 61.63(d, *J* = 6.6 Hz), 68.8 (d, *J* = 138.1 Hz), 75.2 (s), 115.5 (br. s), 127.2 (br. s), 148.7 (s); $^{31}P\{^1H\}$-NMR ($CDCl_3$, 162 MHz): δ 27.61; HRMS (ESI-TOF) m/z: $[M+H]^+$ Calcd for $C_{18}H_{37}N_3O_4P$ 390.2516; Found 390.2516.

4.1.3. Diethyl (1-(*tert*-butyl(1-(1-methyl-1*H*-imidazol-2-yl)ethoxy)amino)-2,2-dimethylpropyl)phosphonate ((*RR/SS*)-2b and (*RS/SR*)-2b). To a stirred solution of salen ligand (0.27 g, 1.0 mmol, 0.05 eq.) in *i*-PrOH (15 mL) was added $MnCl_2$ (0.13 g, 1.0 mmol, 0.05 eq.) in an opened flask. After stirring with air bubbling at rt for 10 min, a solution of SG1 nitroxide (5.89 g, 20 mmol, 1.0 eq.) and 1-methyl-2-vinyl-1*H*-imidazole [28] (2.49 g, 23 mmol, 1.2 eq.) in *i*-PrOH (25 mL) was added, followed by solid $NaBH_4$ (0.76 g, 20 mmol, 1.0 eq.) added in small portions below 25 ºC. The mixture was stirred at rt for 6 h, and the solvent was removed *in vacuo*. Then sat. $NaHCO_3$ and CH_2Cl_2 were added and extracted with CH_2Cl_2. The combined organic phase was washed with brine, dried with $MgSO_4$, and concentrated to afford a crude product as a 2.4: 1 mixture of diastereoisomers (^{31}P-NMR ratio). The crude was separated by flash column chromatography (CH_2Cl_2: acetone = 85: 15 to 50: 50) to afford (*RR/SS*)-**2b** (1.50 g, 19%) and (*RS/SR*)-**2b** (3.11 g, 39%). (*RR/SS*)-**2b**: pale yellow oil; R_f = 0.33 (CH_2Cl_2: acetone = 1: 4); ^1H-NMR ($CDCl_3$, 400 MHz): δ 0.84 (s, 9 H), 1.24 (s, 9 H), 1.31 (t, *J* = 7.1 Hz, 6 H), 1.69 (d, *J* = 7.1 Hz, 3 H), 3.32 (d, *J* = 25.4 Hz, 1 H), 3.78 (s, 3 H), 3.91 - 4.03 (m, 1 H), 4.03 - 4.11 (m, 1 H), 4.11 - 4.22 (m, 1 H), 4.24 - 4.37 (m, 1 H), 5.34 (q, *J* = 7.0 Hz, 1 H), 6.74 (d, *J* = 1.0 Hz, 1 H), 6.97 (d, *J* = 1.0 Hz, 1 H); $^{13}C\{^1H\}$-NMR ($CDCl_3$, 75 MHz): δ 15.8 (d, *J* = 6.6 Hz), 16.2 (d, *J* = 6.1 Hz), 19.9 (s), 27.4 (s), 29.5

(d, *J* = 5.5 Hz), 32.7 (s), 35.1 (d, *J* = 5.5 Hz), 58.6 (d, *J* = 7.7 Hz), 61.21 (d, *J* = 6.1 Hz), 61.22 (s), 70.2 (d, *J* = 138.1 Hz), 75.7 (s), 120.2 (s), 127.0 (s), 149.2 (s); $^{31}P\{^{1}H\}$-NMR ($CDCl_3$, 162 MHz): δ 25.45; HRMS (ESI-TOF) m/z: $[M+H]^+$ Calcd for $C_{19}H_{39}N_3O_4P$ 404.2673; Found 404.2672. (*RS/SR*)-**2b**: pale yellow oil; R_f = 0.43 (CH_2Cl_2: acetone = 1: 4); ^{1}H-NMR ($CDCl_3$, 400 MHz): δ 1.00 (t, *J* = 7.1 Hz, 3 H), 1.21 (s, 18 H), 1.26 (t, *J* = 7.2 Hz, 3 H), 1.67 (d, *J* = 6.6 Hz, 3 H), 3.24 - 3.41 (m, 2 H), 3.39 (d, *J* = 25.7 Hz, 1 H), 3.84 (s, 3 H), 3.85 - 3.93 (m, 1 H), 3.93 - 4.05 (m, 1 H), 5.36 (q, *J* = 6.6 Hz, 1 H), 6.73 (d, *J* = 0.9 Hz, 1 H), 7.02 (d, *J* = 0.7 Hz, 1 H); $^{13}C\{^{1}H\}$-NMR ($CDCl_3$, 75 MHz): δ 15.7 (d, *J* = 7.2 Hz), 16.0 (d, *J* = 6.1 Hz), 18.5 (s), 27.8 (s), 29.8 (d, *J* = 6.1 Hz), 32.5 (s), 34.8 (d, *J* = 5.5 Hz), 58.2 (d, *J* = 7.7 Hz), 60.5 (d, *J* = 6.1 Hz), 61.0 (s), 68.0 (s), 69.9 (d, *J* = 138.6 Hz), 119.8 (s), 127.5 (s), 147.3 (s); $^{31}P\{^{1}H\}$-NMR ($CDCl_3$, 162 MHz): δ 25.06; HRMS (ESI-TOF) m/z: $[M+H]^+$ Calcd for $C_{19}H_{39}N_3O_4P$ 404.2673; Found 404.2671.

4.1.4. 2-(1-((*tert*-Butyl(1-(diethoxyphosphoryl)-2,2-dimethylpropyl)amino)oxy)ethyl)-1,3-dimethyl-1*H*-imidazol-3-ium 4-methylbenzenesulfonate ((*RR/SS*)-2c). To a stirred solution of (*RR/SS*)-**2b** (0.45 g, 1.1 mmol) in THF (3 mL), a solution of methyl *p*-toluenesulfonate (1.2 mL, 1.0 M in THF) was added. The mixture was stirred at rt for 1 d under argon, and then the solvent was removed *in vacuo*. This residue was triturated with pentane/ Et_2O (1:1) and the solvent was removed and dried *in vacuo* to afford (*RR/SS*)-**2c** (0.61 g, 92%). pale yellow oil; ^{1}H-NMR ($CDCl_3$, 400 MHz) δ 0.88 (br. s, 9 H), 1.18 (s, 9 H), 1.33 (t, *J* = 7.1 Hz, 6 H), 1.76 (d, *J* = 7.3 Hz, 3 H), 2.33 (s, 3 H), 3.31 (d, *J* = 25.7 Hz, 1 H), 4.01 (s, 6 H), 3.90 - 4.14 (m, 3 H), 4.15 - 4.27 (m, 1 H), 5.36 - 5.53 (m, 1 H), 7.13 (d, *J* = 7.8 Hz, 2 H), 7.75 (d, *J* = 8.2 Hz, 2 H), 7.77 (s, 2 H); $^{13}C\{^{1}H\}$-NMR ($CDCl_3$, 75 MHz) δ 15.7 (d, *J* = 6.6 Hz), 16.1 (d, *J* = 5.5 Hz), 18.5 (s), 20.7 (s), 27.5 (s), 29.4 (d, *J* = 5.5 Hz), 35.1 (d, *J* = 4.4 Hz), 35.4 (s), 59.9 (d, *J* = 7.7 Hz), 61.2 (d, *J* = 6.6 Hz), 61.8 (s), 69.5 (d, *J* = 142.0 Hz), 74.6 (br. s), 123.6 (s), 125.4 (s), 128.1 (s), 138.8 (s), 143.0 (s), 144.9 (s); $^{31}P\{^{1}H\}$-NMR

($CDCl_3$, 162 MHz): δ 23.81; HRMS (ESI-TOF) m/z: $[M\text{-}TsO^-]^+$ Calcd for $C_{20}H_{41}N_3O_4P$ 418.2829; Found 418.2828.

4.1.5. 2-(1-((*tert*-Butyl(1-(diethoxyphosphoryl)-2,2-dimethylpropyl)amino)oxy)ethyl)-1,3-dimethyl-1*H*-imidazol-3-ium 4-methylbenzenesulfonate ((*RS/SR*)-2c). (*RS/SR*)-**2c** was synthesized in a same procedure as (*RR/SS*)-**2c** with (*RS/SR*)-**2b** (0.41 g, 1.0 mmol) and methyl *p*-toluenesulfonate (1.0 mL, 1.0 M in THF) to give (*RS/SR*)-**2c** (0.29 g, 48%). white solid; m.p.: 120ºC (dec.); ^{1}H-NMR ($CDCl_3$, 400 MHz): δ 1.15 (t, *J* = 7.0 Hz, 3 H), 1.18 (s, 9 H), 1.21 (s, 9 H), 1.29 (t, *J* = 7.0 Hz, 3 H), 1.67 (d, *J* = 7.1 Hz, 3 H), 2.33 (s, 3 H), 3.49 (d, *J* = 27.6 Hz, 1 H), 3.48 - 3.60 (m, 2 H), 3.86 - 4.03 (m, 2 H), 4.05 (s, 6 H), 5.44 (q, *J* = 7.0 Hz, 1 H), 7.13 (d, *J* = 7.9 Hz, 2 H), 7.70 (s, 2 H), 7.78 (d, *J* = 8.1 Hz, 2 H); ^{13}C{^{1}H}-NMR ($CDCl_3$, 75 MHz): δ 15.7 (d, *J* = 6.6 Hz), 16.0 (d, *J* = 5.0 Hz), 16.3 (s), 20.8 (s), 27.7 (s), 30.4 (d, *J* = 5.5 Hz), 34.8 (d, *J* = 3.9 Hz), 36.0 (s), 59.8 (d, *J* = 7.2 Hz), 60.5 (d, *J* = 7.2 Hz), 61.5 (s), 68.1 (d, *J* = 139.8 Hz), 69.3 (s), 123.6 (s), 125.5 (s), 128.0 (s), 138.5 (s), 143.6 (s), 143.7 (s); ^{31}P{^{1}H}-NMR ($CDCl_3$, 162 MHz): δ 23.59; HRMS (ESI-TOF) m/z: $[M\text{-}TsO^-]^+$ Calcd for $C_{20}H_{41}N_3O_4P$ 418.2829; Found 418.2829.

4.1.6. Diethyl (1-((1-(1*H*-imidazol-1-yl)ethoxy)(*tert*-butyl)amino)-2,2-dimethylpropyl)phosphonate ((*RR/SS*)-3a and (*RS/SR*)-3a). To a stirred solution of salen ligand (0.27 g, 1.0 mmol, 0.05 eq.) in *i*-PrOH (15 mL) was added $MnCl_2$ (0.13 g, 1.0 mmol, 0.05 eq.) in an opened flask. After stirring with air bubbling at rt for 10 min, a solution of SG1 nitroxide (5.89 g, 20 mmol, 1.0 eq.) and 1-vinyl-1*H*-imidazole (2.82 g, 30 mmol, 1.5 eq.) in *i*-PrOH (25 mL) was added, followed by solid $NaBH_4$ (0.76 g, 20 mmol, 1.0 eq.) added in small portions below 25 ºC. The mixture was stirred at rt for 2.5 h, and the solvent was removed *in vacuo*. Then sat. $NaHCO_3$ and CH_2Cl_2 were added and extracted with CH_2Cl_2. The combined organic phase was washed with brine, dried with $MgSO_4$, and concentrated to afford a crude product as a 1.25: 1 mixture of diastereoisomers (^{31}P-NMR ratio). The crude

was separated by flash column chromatography (CH_2Cl_2: MeOH = 97: 3) to afford (*RR/SS*)-**3a** (1.47 g, 19%) and (*RS/SR*)-**3a** (1.40 g, 18%). (*RR/SS*)-**3a**: pale yellow oil. R_f = 0.23 (CH_2Cl_2: MeOH = 19: 1); ^{1}H-NMR ($CDCl_3$, 400 MHz): δ 0.78 (s, 9 H), 1.26 (s, 9 H), 1.33 (t, *J* = 7.1 Hz, 3 H), 1.34 (t, *J* = 7.1 Hz, 3 H), 1.78 (d, *J* = 6.1 Hz, 3 H), 3.39 (d, *J* = 26.7 Hz, 1 H), 3.94 - 4.05 (m, 1 H), 4.05 - 4.17 (m, 2 H), 4.29 (dquint, *J* = 10.3, 7.3, 7.3, 7.3, 7.3 Hz, 1 H), 5.86 (q, *J* = 6.1 Hz, 1 H), 7.03 (s, 1 H), 7.08 (s, 1 H), 7.72 (s, 1 H); ^{13}C{^{1}H}-NMR ($CDCl_3$, 75 MHz): δ 15.9 (d, *J* = 6.6 Hz), 16.2 (d, *J* = 6.1 Hz), 19.8 (s), 26.6 (s), 30.5 (d, *J* = 6.1 Hz), 35.0 (d, *J* = 5.0 Hz), 59.1 (d, *J* = 7.2 Hz), 61.17 (d, *J* = 7.2 Hz), 61.23 (s), 69.1 (d, *J* = 139.8 Hz), 84.8 (s), 117.0 (s), 128.5 (s), 136.7 (s); ^{31}P{^{1}H}-NMR ($CDCl_3$, 162 MHz): δ 24.49; HRMS (ESI-TOF) m/z: $[M+H]^+$ Calcd for $C_{18}H_{37}N_3O_4P$ 390.2516; Found 390.2520. (*RS/SR*)-**3a**: white crystal (recrystallized from EtOAc); m.p.: 68-70°C; R_f = 0.17 (CH_2Cl_2: MeOH = 19: 1); ^{1}H-NMR (DMSO-d_6, 500 MHz, 369 K): δ 1.09 (s, 9 H), 1.11 (s, 9 H), 1.14 (t, *J* = 7.3 Hz, 3 H), 1.26 (t, *J* = 7.0 Hz, 3 H), 1.67 (d, *J* = 6.4 Hz, 3 H), 3.37 (d, *J* = 25.0 Hz, 1 H), 3.60 - 4.07 (m, 4 H), 6.10 (q, *J* = 6.1 Hz, 1 H), 6.86 (s, 1 H), 7.32 (s, 1 H), 7.83 (s, 1 H); ^{13}C{^{1}H}-NMR ($CDCl_3$, 75 MHz): δ 16.0 (d, *J* = 6.6 Hz), 16.1 (d, *J* = 6.1 Hz), 19.4 (s), 27.7 (s), 30.1 (br. s), 35.0 (br. s), 58.9 (br. s), 60.6 (br. s), 61.5 (s), 69.3 (d, *J* = 140.3 Hz), 83.2 (br. s), 117.1 (br. s), 128.6 (br. s), 137.0 (br. s); ^{31}P{^{1}H}-NMR ($CDCl_3$, 162 MHz): δ 23.91; HRMS (ESI-TOF) m/z: $[M+H]^+$ Calcd for $C_{18}H_{37}N_3O_4P$ 390.2516; Found 390.2519.

4.1.7. 1-(1-((*tert*-Butyl(1-(diethoxyphosphoryl)-2,2-dimethylpropyl)amino)oxy)ethyl)-3-methyl-1*H*-imidazol-3-ium 4-methylbenzenesulfonate ((*RR/SS*)-3b). (*RR/SS*)-**3b** was synthesized using same procedure as (*RR/SS*)-**2c** with (*RR/SS*)-**3a** (0.30 g, 0.77 mmol) and methyl *p*-toluenesulfonate (0.7 mL, 1.0 M in THF) to give (*RR/SS*)-**3b** (0.35 g, 79%). Pale yellow oil; ^{1}H-NMR ($CDCl_3$, 400 MHz): δ 0.79 (s, 9 H), 1.19 (s, 9 H), 1.29 (t, *J* = 7.1 Hz, 3 H), 1.32 (t, *J* = 7.1 Hz, 3 H), 1.88 (d, *J* = 6.1 Hz, 3 H), 2.32 (s, 3 H), 3.35 (d, *J* = 27.0 Hz, 1 H), 3.93 - 4.14 (m, 3 H), 4.09 (s, 3 H), 4.22 (dquint, *J* = 10.2, 7.3, 7.3, 7.3, 7.3 Hz, 1 H), 5.97

(q, *J* = 6.1 Hz, 1 H), 7.12 (d, *J* = 7.9 Hz, 2 H), 7.36 (d, *J* = 1.6 Hz, 1 H), 7.54 (s, 1 H), 7.76 (d, *J* = 8.2 Hz, 2 H), 9.96 (s, 1 H); $^{13}C\{^{1}H\}$-NMR ($CDCl_3$, 75 MHz): δ 15.9 (d, *J* = 6.6 Hz), 16.2 (d, *J* = 5.5 Hz), 19.9 (s), 20.9 (s), 26.8 (s), 30.3 (d, *J* = 5.5 Hz), 35.0 (d, *J* = 4.4 Hz), 36.2 (s), 59.5 (d, *J* = 7.7 Hz), 61.5 (d, *J* = 6.6 Hz), 61.6 (s), 69.0 (d, *J* = 140.3 Hz), 88.9 (s), 120.6 (s), 123.7 (s), 125.6 (s), 128.2 (s), 136.9 (s), 138.8 (s), 143.8 (s); $^{31}P\{^{1}H\}$-NMR ($CDCl_3$, 162 MHz): δ 23.32; HRMS (ESI-TOF) m/z: $[M\text{-}TsO^-]^+$ Calcd for $C_{19}H_{39}N_3O_4P$ 404.2673; Found 404.2675.

4.1.8. 1-(1-((*tert*-Butyl(1-(diethoxyphosphoryl)-2,2-dimethylpropyl)amino)oxy)ethyl)-3-methyl-1*H*-imidazol-3-ium 4-methylbenzenesulfonate ((*RS/SR*)-3b). (*RS/SR*)-**3b** was synthesized using same procedure as (*RR/SS*)-**2c** with (*RS/SR*)-**3a** (0.35 g, 0.90 mmol) and methyl *p*-toluenesulfonate (0.94 mL, 1.0 M in THF) to give (*RS/SR*)-**3b** (0.10 g, 19%). White solid; m.p.: 114-116ºC; ^{1}H-NMR ($CDCl_3$, 400 MHz): δ 0.85 (br. s, 9 H), 1.21 (br. s, 9 H), 1.32 (t, *J* = 7.0 Hz, 6 H), 1.77 (d, *J* = 6.0 Hz, 3 H), 2.34 (s, 3 H), 3.26 (d, *J* = 27.1 Hz, 1 H), 3.89 - 4.11 (m, 2 H), 4.03 (br. s, 3 H), 4.12 - 4.29 (m, 2 H), 6.29 (br. s, 1 H), 7.14 (d, *J* = 7.9 Hz, 2 H), 7.19 (br. s, 1 H), 7.81 (d, *J* = 8.2 Hz, 2 H), 7.98 (s, 1 H), 10.13 (s, 1 H); $^{13}C\{^{1}H\}$-NMR ($CDCl_3$, 75 MHz): δ 15.8 (d, *J* = 7.2 Hz), 16.0 (d, *J* = 6.1 Hz), 20.8 (s), 21.0 (br. s), 27.4 (s), 29.2 (br. s), 34.8 (br. s), 36.0 (s), 59.4 (br. s), 61.3 (d, *J* = 7.2 Hz), 63.0 (br. s), 67.6 (d, *J* = 135.9 Hz), 89.2 (br. s), 121.5 (br. s), 122.6 (s), 125.5 (s), 128.0 (s), 136.9 (s), 138.4 (s), 143.9 (s); $^{31}P\{^{1}H\}$-NMR ($CDCl_3$, 162 MHz): δ 24.03; HRMS (ESI-TOF) m/z: $[M\text{-}TsO^-]^+$ Calcd for $C_{19}H_{39}N_3O_4P$ 404.2673; Found 404.2676.

4.1.9. Diethyl (1-((1-(1*H*-imidazol-4-yl)ethoxy)(*tert*-butyl)amino)-2,2-dimethylpropyl)phosphonate ((*RR/SS*)-4a and (*RS/SR*)-4a). To a stirred solution of salen ligand (0.23 g, 0.9 mmol, 0.05 eq.) in *i*-PrOH (15 mL) was added $MnCl_2$ (0.11 g, 0.9 mmol, 0.05 eq.) in an opened flask. After stirring with air bubbling at rt for 10 min, a solution of SG1 nitroxide (5.09 g, 17 mmol, 1.0 eq.) and 4-vinyl-1*H*-imidazole [29] (1.87 g, 20 mmol,

1.2 eq.) in *i*-PrOH (25 mL) was added, followed by solid $NaBH_4$ (0.75 g, 20 mmol, 1.2 eq.) added in small portions below 25 °C. The mixture was stirred at rt for 5.5 h, and the solvent was removed *in vacuo*. Then sat. $NaHCO_3$ and CH_2Cl_2 were added and extracted with CH_2Cl_2. The combined organic phase was washed with brine, dried with $MgSO_4$, and concentrated to afford a crude product as a 1: 1 mixture of diastereoisomers (^{31}P-NMR ratio). The crude was separated by flash column chromatography (CH_2Cl_2: MeOH = 100: 0 to 9: 1) to afford (*RR/SS*)-**4a** (1.29 g, 19%) and (*RS/SR*)-**4a** (1.38 g, 20%). (*RR/SS*)-**4a**: pale yellow solid; m.p.: 36-38°C; R_f = 0.35 (CH_2Cl_2: MeOH = 9: 1); ^{1}H-NMR ($CDCl_3$, 400 MHz): δ 1.05 (s, 9 H), 1.19 (t, *J* = 7.1 Hz, 3 H), 1.25 (s, 9 H), 1.34 (t, *J* = 7.1 Hz, 3 H), 1.70 (d, *J* = 6.6 Hz, 3 H), 3.37 (d, *J* = 27.4 Hz, 1 H), 3.73 - 3.87 (m, 1 H), 3.93 - 4.07 (m, 2 H), 4.07 - 4.20 (m, 1 H), 5.13 (q, *J* = 6.6 Hz, 1 H), 6.91 (s, 1 H), 7.56 (s, 1 H); ^{13}C{^{1}H}-NMR ($CDCl_3$, 75 MHz): δ 16.0 (d, *J* = 6.6 Hz), 16.2 (d, *J* = 6.6 Hz), 20.2 (s), 27.5 (s), 30.5 (d, *J* = 6.1 Hz), 35.1 (d, *J* = 4.4 Hz), 59.0 (d, *J* = 7.2 Hz), 61.27 (d, *J* = 6.0 Hz), 61.30 (s), 69.5 (d, *J* = 139.7 Hz), 73.7 (s), 121.2 (br. s), 134.6 (br. s), 136.2 (br. s); ^{31}P{^{1}H}-NMR ($CDCl_3$, 162 MHz): δ 26.45; HRMS (ESI-TOF) m/z: $[M+H]^+$ Calcd for $C_{18}H_{37}N_3O_4P$ 390.2516; Found 390.2514. (*RS/SR*)-**4a**: pale yellow solid; m.p.: 100-102°C; R_f = 0.47 (CH_2Cl_2: MeOH = 9: 1); ^{1}H-NMR ($CDCl_3$, 400 MHz): δ 1.14 (s, 9 H), 1.17 (s, 9 H), 1.20 (t, *J* = 7.1 Hz, 3 H), 1.36 (t, *J* = 7.1 Hz, 3 H), 1.62 (d, *J* = 6.6 Hz, 3 H), 3.48 (d, *J* = 27.9 Hz, 1 H), 3.73 - 3.85 (m, 1 H), 3.92 - 4.09 (m, 2 H), 4.09 - 4.21 (m, 1 H), 5.11 (q, *J* = 6.6 Hz, 1 H), 7.01 (s, 1 H), 7.54 (s, 1 H); ^{13}C{^{1}H}-NMR ($CDCl_3$, 75 MHz): δ 15.9 (d, *J* = 3.3 Hz), 16.0 (d, *J* = 2.8 Hz), 17.6 (s), 27.8 (s), 30.7 (d, *J* = 5.5 Hz), 35.0 (d, *J* = 5.0 Hz), 59.4 (d, *J* = 7.7 Hz), 60.8 (s), 61.6 (d, *J* = 6.6 Hz), 69.0 (d, *J* = 138.6 Hz), 70.4 (s), 125.7 (br. s), 130.9 (br. s), 134.8 (s); ^{31}P{^{1}H}-NMR ($CDCl_3$, 162 MHz): δ 27.59; HRMS (ESI-TOF) m/z: $[M+H]^+$ Calcd for $C_{18}H_{37}N_3O_4P$ 390.2516; Found 390.2515.

4.1.9. Diethyl (1-(*tert*-butyl(1-(1-methyl-1*H*-imidazol-4-yl)ethoxy)amino)-2,2-dimethylpropyl)phosphonate ((*RR/SS*)-4b) and 4-(1-((*tert*-butyl(1-(diethoxyphosphoryl)-

2,2-dimethylpropyl)amino)oxy)ethyl)-1,3-dimethyl-1*H*-imidazol-3-ium iodide ((*RR/SS*)-4c). To a stirred solution of (*RR/SS*)-**4a** (0.26 g, 0.67 mmol) in CH_2Cl_2 (5 mL), K_2CO_3 (0.18 g, 1.31 mmol) and MeI (82 μL, 1.31 mmol) were added. The mixture was stirred at rt for 1 d under argon, and then the solvent was removed *in vacuo*. This residue was triturated with Et_2O and the precipitate was filtered off to afford (*RR/SS*)-**4c** (0.12 g, 46%). The filtrate was concentrated *in vacuo* to afford (*RR/SS*)-**4b** (0.17 g, 48%). The assignment is supported by an X-ray crystallographic structure determination. (*RR/SS*)-**4b**: pale yellow crystal (recrystallized from EtOAc); m.p.: 64-66 ºC; R_f = 0.43 (CH_2Cl_2: MeOH = 9: 1); ^{1}H-NMR ($CDCl_3$, 400 MHz): δ 0.85 (s, 9 H), 1.24 (s, 9 H), 1.29 (t, *J* = 7.1 Hz, 3 H), 1.32 (t, *J* = 7.2 Hz, 3 H), 1.61 (d, *J* = 6.6 Hz, 3 H), 3.37 (d, *J* = 26.2 Hz, 1 H), 3.66 (s, 3 H), 3.97 (dquint, *J* = 10.1, 7.0, 7.0, 7.0, 7.0 Hz, 1 H), 4.03 - 4.20 (m, 2 H), 4.30 (dquint, *J* = 10.4, 7.3, 7.3, 7.3, 7.3 Hz, 1 H), 5.04 (q, *J* = 6.6 Hz, 1 H), 6.82 (d, *J* = 1.2 Hz, 1 H), 7.35 (s, 1 H); ^{13}C{^{1}H}-NMR ($CDCl_3$, 75 MHz): δ 15.6 (d, *J* = 6.6 Hz), 15.8 (d, *J* = 6.6 Hz), 19.3 (s), 27.2 (s), 30.0 (d, *J* = 5.5 Hz), 32.6 (s), 34.6 (d, *J* = 5.5 Hz), 58.1 (d, *J* = 7.2 Hz), 60.3 (s), 60.8 (d, *J* = 6.6 Hz), 69.2 (d, *J* = 138.6 Hz), 74.7 (s), 118.0 (s), 135.9 (s), 143.7 (s); ^{31}P{^{1}H}-NMR ($CDCl_3$, 162 MHz): δ 25.44; HRMS (ESI-TOF) m/z: $[M+H]^+$ Calcd for $C_{19}H_{39}N_3O_4P$ 404.2673; Found 404.2675. (*RR/SS*)-**4c**: yellow oil; ^{1}H-NMR ($CDCl_3$, 400 MHz): δ 0.97 (br. s, 9 H), 1.21 (s, 9 H), 1.33 (t, *J* = 7.1 Hz, 6 H), 1.75 (d, *J* = 7.0 Hz, 3 H), 3.36 (d, *J* = 26.3 Hz, 1 H), 4.13 (s, 3 H), 4.07 (s, 3 H), 3.93 - 4.29 (m, 4 H), 5.14 - 5.29 (m, 1 H), 7.18 (s, 1 H), 10.08 (s, 1 H); ^{13}C{^{1}H}-NMR ($CDCl_3$, 75 MHz): δ 15.9 (d, *J* = 6.6 Hz), 16.3 (d, *J* = 5.5 Hz), 20.9 (s), 28.0 (s), 30.0 (d, *J* = 5.5 Hz), 35.2 (d, *J* = 5.0 Hz), 35.5 (s), 37.1 (s), 59.6 (d, *J* = 7.7 Hz), 61.4 (d, *J* = 6.6 Hz), 61.8 (s), 69.5 (d, *J* = 144.2 Hz), 73.6 (br. s), 121.1 (br. s), 137.2 (s), 137.4 (s); ^{31}P{^{1}H}-NMR ($CDCl_3$, 162 MHz): δ 24.38; HRMS (ESI-TOF) m/z: $[M+H]^+$ Calcd for $C_{20}H_{41}N_3O_4P$ 418.2829; Found 418.2829.

4.1.10. Diethyl (1-(*tert*-butyl(1-(1-methyl-1*H*-imidazol-4-yl)ethoxy)amino)-2,2-dimethylpropyl)phosphonate ((*RS/SR*)-4b) and 4-(1-((*tert*-butyl(1-(diethoxyphosphoryl)-2,2-dimethylpropyl)amino)oxy)ethyl)-1,3-dimethyl-1*H*-imidazol-3-ium iodide ((*RS/SR*)-4c). (*RS/SR*)-**4b** and (*RS/SR*)-**4c** were synthesized according to the same procedure as (*RR/SS*)-**4b** and (*RR/SS*)-**4c** with (*RS/SR*)-**4a** (0.28 g, 0.72 mmol), K_2CO_3 (0.20 g, 1.41 mmol) and MeI (88 μL, 1.41 mmol). (*RS/SR*)-**4b**: Yield: 88 mg (31%); yellow solid; m.p.: 88-90 ºC; R_f = 0.48 (CH_2Cl_2: MeOH = 9: 1); ^{1}H-NMR ($CDCl_3$, 400 MHz): δ 1.06 (t, *J* = 7.1 Hz, 3 H), 1.18 (s, 18 H), 1.26 (t, *J* = 7.0 Hz, 3 H), 1.61 (d, *J* = 6.6 Hz, 3 H), 3.40 (d, *J* = 26.5 Hz, 1 H), 3.62 (s, 3 H), 3.50 - 3.68 (m, 1 H), 3.69 - 3.84 (m, 1 H), 3.84 - 4.08 (m, 2 H), 5.23 (q, *J* = 6.6 Hz, 1 H), 7.08 (s, 1 H), 7.38 (s, 1 H); ^{13}C{^{1}H}-NMR ($CDCl_3$, 75 MHz): δ 15.6 (d, *J* = 7.2 Hz), 15.8 (d, *J* = 6.1 Hz), 18.4 (s), 27.6 (s), 30.0 (d, *J* = 5.5 Hz), 32.7 (s), 34.7 (d, *J* = 5.0 Hz), 58.3 (d, *J* = 7.7 Hz), 60.5 (s), 61.0 (d, *J* = 6.1 Hz), 69.7 (d, *J* = 139.8 Hz), 71.8 (s), 118.9 (s), 136.1 (s), 142.6 (s); ^{31}P{^{1}H}-NMR ($CDCl_3$, 162 MHz): δ 25.14; HRMS (ESI-TOF) m/z: $[M+H]^+$ Calcd for $C_{19}H_{39}N_3O_4P$ 404.2673; Found 404.2674. (*RS/SR*)-**4c**: Yield: 104 mg (27%); pale yellow powder; m.p.: 160 ºC (dec.); ^{1}H-NMR ($CDCl_3$, 400 MHz): δ 1.12 (s, 9 H), 1.19 (t, *J* = 7.1 Hz, 3 H), 1.19 (s, 9 H), 1.29 (t, *J* = 7.1 Hz, 3 H), 1.62 (d, *J* = 6.7 Hz, 3 H), 3.41 (d, *J* = 26.7 Hz, 1 H), 3.52 - 3.66 (m, 1 H), 3.66 - 3.80 (m, 1 H), 3.86 - 3.98 (m, 1 H), 4.05 (s, 3 H), 3.98 - 4.08 (m, 1 H), 4.09 (s, 3 H), 5.25 (q, *J* = 6.7 Hz, 1 H), 7.29 (d, *J* = 1.6 Hz, 1 H), 10.22 (s, 1 H); ^{13}C{^{1}H}-NMR ($CDCl_3$, 75 MHz): δ 15.6 (d, *J* = 7.2 Hz), 16.0 (d, *J* = 5.5 Hz), 20.2 (s), 27.6 (s), 29.9 (d, *J* = 5.5 Hz), 34.4 (s), 34.6 (d, *J* = 4.4 Hz), 36.6 (s), 59.1 (d, *J* = 7.7 Hz), 60.8 (d, *J* = 6.6 Hz), 61.2 (s), 68.6 (d, *J* = 141.4 Hz), 68.5 (s), 121.2 (s), 136.0 (s), 136.4 (s); ^{31}P{^{1}H}-NMR ($CDCl_3$, 162 MHz): δ 23.80; HRMS (ESI-TOF) m/z: $[M+H]^+$ Calcd for $C_{20}H_{41}N_3O_4P$ 418.2829; Found 418.2831.

4.2. p*K*$_a$ measurement. p*K*$_a$ values of **2a-b**, **3a** and **4a-b** were measured by monitoring the dependency of ^{1}H NMR chemical shift at various pH. A 0.01 M solution of alkoxyamine in

D_2O/CD_3OD (1/1) was used. The pH* values, where the asterisk (*) means that the pH was measured in D_2O/CD_3OD using a pH-meter calibrated with non-deuterated standard solutions, were adjusted with DCl and NaOD to various pH values and ^{1}H-NMR spectra were recorded on a 400 MHz NMR spectrometer. The chemical shift of proton signals on the imidazole ring was plotted against pH* (see Figure S1-S5 in supplementary data) and a sigmoidal fitting was performed. The obtained pK_a* from the curve fitting - which value was determined from pH* - was then corrected to pK_a using the following equation pH = 0.929 pH* + 0.42 [11].

4.3. Kinetics measurement. The values of homolysis rate constants k_d of **2a-c** and **4a-c** were determined by monitoring the concentration of nitroxide by EPR. A sample tube containing a solution of 1 x 10^{-4} M of alkoxyamine in H_2O/MeOH (1:1) buffered with $Na_2CO_3/NaHCO_3$ for pH = 10.3, 50 mM HEPES buffer containing 0.15 mM NaCl for pH 7.4 or HCl/KCl for pH = 2.2 was set in EPR cavity and EPR spectrum were recorded sequentially. The temperature in the cavity was controlled by a temperature controlling unit. The area of the double-integrated signal (I) was plotted against time, and the curve fitting was performed by the exponential fitting to obtain the plateau value (I_∞) of the double-integrated signal. Then, the value of $\ln\{(I_\infty - I) / I_\infty\}$ was plotted against time, and this plot was fitted by linear regression to give the k_d value. The k_d values of **3a-b** were determined by monitoring the decay of alkoxyamine by $^{31}P\{^1H\}$-NMR in the presence of TEMPOL (4-hydroxy-2,2,6,6-tetramethylpiperidin-*N*-oxyl) as alkyl radical scavenger to avoid the reverse reaction for the production of the alkoxyamine. A stock solution of 0.02 M of alkoxyamine in H_2O/MeOH with 2 equiv. of TEMPOL was prepared. Same buffer solutions as EPR measurement were used for specific pH conditions. The stock solution was sampled into 20 NMR tubes (0.5 mL in each tube). They were sunk in a pre-heated oil bath at reaction temperature, then withdrawn at various time intervals and quenched on a ice-water bath. Then 0.1 mL of DMSO-d_6 containing $(EtO)_3PO$ (0.002 M) as internal standard (δ = 0 ppm) was added to each tube.

$^{31}P\{^{1}H\}$-NMR signal was recorded on a 400 MHz NMR spectrometer. The value of ln(*Int* / Int_0), where *Int* is the integral value and Int_0 is the integral value at $t = 0$, was plotted against time and the linear fitting was performed to give the k_d value. In general, more than 90% conversion was reached for both EPR and NMR measurements. The k_d values were then converted to activation energy (E_a) using Arrhenius equation with the averaged frequency factor $A = 2.4.10^{14}$ s^{-1}. The half-life time $t_{1/2}$ was calculated from the following equation, $t_{1/2} = \ln 2 / k_d$.

4.4. Cell Cultures. Human glioblastoma cell lines U87-MG an U251-MG were cultured in Dulbecco's modified Eagle's medium (DMEM) and Eagle's minimum essential medium (EMEM), respectively, supplemented with 10% fetal bovine serum (FBS), 100 U/mL of Penicillin and 100 µg/mL of Streptomycin (Pen Strep). EMEM was additionally supplemented with 2 µM of L-glutamine. Cell lines were regularly screened and are free from mycoplasma contamination.

4.5. Viability assays. Stock solutions of each alkoxyamine were prepared in DMSO at 0.15 M. Cells were treated with a range of concentrations of alkoxyamines (500, 250, 100, 50, 25, 10 and 5 µM) for 72 h. The highest concentration of DMSO of which cells were exposed to was 0.002%. Cells were seeded in 96-well plates (5000 cells/plate) and treated with alkoxyamines. After a 72 h-treatment, cell survival was measured by incubating the glioblastoma cells for 1 h in the medium replenished with 0.5 mg/mL of MTT (3-(4,5-dimethylthiazol-2-yl)-2,5-diphenyl tetrazolium bromide). Medium was replaced by DMSO and optical density (OD) was measured by a microplate spectrophotometer at 550 nm. For each dose of each alkoxyamine tested, results were expressed as percentage of survival cells, according to the following equation: $OD_{treated\ cells} \times 100/OD_{control\ cells}$. The IC_{50} values, *i.e.* concentrations that inhibit 50% of cell survival, were graphically determined. All experiments were performed at least in triplicate. The viability test in the presence of alkyl scavenger was

carried out with an IC_{50} concentrations of alkoxyamines and an incubation time of 72h. U87-MG and U251-MG cell viability was measured *versus* equal concentrations of the nontoxic radical scavenger trihydroxyethylrutin (Troxerutin). Images of the treated cells were captured with a camera on an inverted light microscope.

4.6. $LogD_{7.4}$ measurements. $LogD_{7.4}$ values were determined by standard shake-flask procedure using pre-saturated solutions (*n*-octanol and PBS at pH 7.4). Aqueous phases were then analyzed by RP-HPLC (column: 4.6 × 50 mm, 2.7 µM; solvent: CH_3CN (+ 0.1% TFA) / H_2O (+ 0.1% TFA), 10:90 to 100/0 in 10 min).

Acknowledgements

The authors were financially supported by Aix-Marseille Université, Centre National de la Recherche Scientifique (CNRS), Institut National de la Santé et de la Recherche Médicale (INSERM) and Assistance Publique des Hôpitaux de Marseille (APHM). The project leading to this publication has received funding from Excellence Initiative of Aix-Marseille University - A*MIDEX, a French "Investissements d'Avenir" program, from the *Fondation ARC pour la recherche sur le cancer* (nº PJA 20141201886), and from DGOS (SIRIC label) INCa-DGOS-INSERM 6038. This work was also supported by the foundations ReSOP "*Réseau d'Onco-hématologie Pédiatrique*" and AROU "*Association pour la Recherche en Oncologie pédiatrique et Urologique*", as well as by the computing facilities of the CRCMM '*Centre Régional de Compétences en Modélisation Moléculaire de Marseille*'. The authors thank Pr. Didier Siri for his kind assistance. Marie-Pierre Montero is gratefully acknowledged for her help in the culture of cancer cell lines.

Appendix A. Supplementary data

Supplementary material to this article (characterization data, kinetic and pK_a data, calculations details and x-ray crystallographic data) can be found online at .

Notes and references

1 W. J. Geldenhuys, A. S. Mohammad, C. E. Adkins, P. R. Lockman. Molecular determinants of blood-brain barrier permeation. *Ther. Deliv.,* 2015, 6, 961-971.

2 G. Audran, P. Brémond, S. R. A. Marque. Labile alkoxyamines: past, present, and future. *Chem. Commun.*, 2014, 50, 7921-7928.

3 For recent publications about alkoxyamines, see: (a) M. Baron, J. C. Morris, S. Telitel, J.-L. Clément, J. Lalevée, F. Morlet-Savary, A. Spangenberg, J.-P. Malval, O. Soppera, D. Gigmes, Y. Guillaneuf. Light-Sensitive Alkoxyamines as Versatile Spatially- and Temporally- Controlled Precursors of Alkyl Radicals and Nitroxides. *J. Am. Chem. Soc*. 2018, 140, 3339-3344; (b) H. Takeshima, K. Satoh, M. Kamigaito. Bio-Based Functional Styrene Monomers Derived from Naturally Occurring Ferulic Acid for Poly(vinylcatechol) and Poly(vinylguaiacol) via Controlled Radical Polymerization. *Macromolecules*, 2017, 50, 4206-4216; (c) A. Simula, M. Aguirre, N. Ballard, A. Veloso, J. R. Leiza, S. van Es, J. M. Asua. Novel alkoxyamines for the successful controlled polymerization of styrene and methacrylates. *Polym. Chem.*, 2017, 8, 1728-1736; (d) Y.-X. Li, Q.-Q. Wang, L. Yang. Metal-free decarbonylative alkylation-aminoxidation of styrene derivatives with aliphatic aldehydes and N-hydroxyphthalimide. *Org. Biomol. Chem.*, 2017, 15, 1338-1342; (e) D. Le, T. N. T. Phan, L. Autissier, L. Charles, D. Gigmes. A well-defined block copolymer synthesis via living cationic polymerization and nitroxide-mediated polymerization using carboxylic acid-based alkoxyamines as a dual initiator. *Polym. Chem.*, 2016, 7, 1659-1667; (f) S. Bottle, J.-L. Clement, M. Fleige, E. M. Simpson, Y. Guillaneuf, K. E. Fairfull-Smith, D. Gigmes, J. P. Blinco. Light-active azaphenalene alkoxyamines: fast and efficient

mediators of a photo-induced persistent radical effect. *RSC Adv.*, 2016, 6, 80328-80333; (g) Y. Jing, M. Tesch, L. Wang, C. G. Daniliuc, A. Studer. Synthesis of a Bulky Nitroxide and Its Application in the Nitroxide-mediated Radical Polymerization. *Tetrahedron*, 2016, 72, 7665-7671; (h) Q. Zhu, E. C. Gentry, R. R. Knowles. Catalytic Carbocation Generation Enabled by the Mesolytic Cleavage of Alkoxyamine Radical Cations. *Angew. Chem. Int. Ed.*, 2016, 55, 9969-9973.

4 C. Prescott, S. E. Bottle. Biological Relevance of Free Radicals and Nitroxides. *Cell Biochem. Biophys.*, 2017, 75, 227-240.

5 J. Nicolas, Y. Guillaneuf, C. Lefay, D. Bertin, D. Gigmes, B. Charleux. Nitroxide-mediated polymerization. *Prog. Polym. Sci.*, 2013, 38, 63-235.

6 G. Audran, P. Brémond, J.-M. Franconi, S. R. A. Marque, P. Massot, P. Mellet, E. Parzy, T. Thiaudière. Alkoxyamines: a new family of pro-drugs against cancer. Concept for theranostics. *Org. Biomol. Chem.*, 2014, 12, 719-723.

7 D. Moncelet, P. Voisin, V. Bouchaud, P. Massot, E. Parzy, G. Audran, J.-M. Franconi, S. R. A. Marque, P. Brémond, P. Mellet. Alkoxyamines: Toward a New Family of Theranostic Agents against Cancer. *Mol. Pharmaceutics*, 2014, 11, 2412-2419.

8 (a) P. Brémond, A. Koïta, S. R. A. Marque, V. Pesce, V. Roubaud, D. Siri. Chemically triggered C-ON bond homolysis of alkoxyamines. Quaternization of the alkyl fragment. *Org. Lett.*, 2012, 14, 358-361; (b) G. Audran, P. Brémond, S. R. A. Marque, G. Obame. Chemically triggered C-ON bond homolysis of alkoxyamines. 5. Cybotactic effect. *J. Org. Chem.*, 2012, 77, 9634-9640.

9 Some examples of imidazole-containing natural compounds or drugs: histidine, histamine, metronidazole, prochlorazole, benznidazole, etc.

10 CCDC numbers for *(RS/SR)*-**3a**: 1583093; *(RR/SS)*-**4b**: 1583092.

11 All pH measured in D_2O/CD_3OD (1:1 *v/v*) were re-estimated using the following equation: pH = 0.929 × pH* + 0.42. pH* is the pH measured in D_2O/CD_3OD (1:1 *v/v*) solutions using a pH-meter calibrated with non-deuterated buffered solutions. See: A. Krężel, W. J. Bal. A formula for correlating pKa values determined in D_2O and H_2O. *Inorg. Biochem.*, 2004, 98, 161-166.

12 G. Audran, P. Brémond, J.-P. Joly, S. R. A. Marque, T. Yamasaki. C–ON bond homolysis in alkoxyamines. Part 12: the effect of the para-substituent in the 1-phenylethyl fragment. *Org. Biomol. Chem.*, 2016, 14, 3574-3583.

13 E_a values of *(RR/SS)*- and *(RS/SR)*-diastereoisomers of the benchmark secondary alkoxyamine SG1-CH(Ph)CH_3 are 123.0 and 124.0 kJ/mol, respectively, and $t_{1/2}$ (37 °C) values are 18 d and 26 d, respectively. Thereby, at first glance, E_a values of both diastereoisomers of **3** were *ca.* 20 kJ/mol higher than expected.

14 G. Audran, M. Batsiandzy Ibanou, P. Brémond, S. R. A. Marque, G. Obame, V. Roubaud, D. Siri. Chemically triggered C–ON bond homolysis in alkoxyamines. Part 7. Remote polar effect. *J. Phys. Org. Chem.*, 2014, 27, 387-391.

15 Moreover, no anomeric effect, *i.e.* $n_O \rightarrow \sigma^*_{C-N}$, that may significantly strengthen the C–ON bond, was observed on the X-ray structure of (*RS/SR*)-3a, nor on the calculated structures. See (a) M. V. Ciriano, H.-G. Korth, W. B. Van Scheppingen, P. Mulder. Thermal Stability of 2,2,6,6-Tetramethylpiperidine-1-oxyl (TEMPO) and Related N-Alkoxyamines *J. Am. Chem. Soc.*, 1999, 121, 6375-6381; (b) S. Marque, H. Fischer, E. Baier, A. Studer. Factors influencing the C-O bond homolysis of alkoxyamines: effects of H-bonding and polar substituents. *J. Org. Chem.*, 2001, 66, 1146-1156.

16 M. Le Grand, R. Berges, E. Pasquier, M.-P. Montero, L. Borge, A. Carrier, S. Vasseur, V. Bourgarel, D. Buric, N. André, D. Braguer, M. Carré. Akt targeting as a strategy to boost

chemotherapy efficacy in non-small cell lung cancer through metabolism suppression. *Sci. Rep.* 2017, *7*, 45136.

17 E. Denicolaï, N. Baeza-Kallee, A. Tchoghandjian, M. Carré, C. Colin, C. J. Jiglaire, S. Mercurio, S. Beclin, D. Figarella-Branger. Proscillaridin A is cytotoxic for glioblastoma cell lines and controls tumor xenograft growth *in vivo*. *Oncotarget*, 2014, 5, 10934-10948.

18 I. D. Alves, M. Carré, M.-P. Montero, S. Castano, S. Lecomte, R. Marquant, P. Lecorché, F. Burlina, C. Schatz, S. Sagan, G. Chassaing, D. Braguer, S. Lavielle. A proapoptotic peptide conjugated to penetratin selectively inhibits tumor cell growth. *Biochem. Biophys. Acta*, 2014, 1838, 2087-2098.

19 S. Mercurio, L. Padovani, C. Colin, M. Carré, A. Tchoghandjian, D. Scavarda, S. Lambert, N. Baeza-Kallee, C. Ferdandez, C. Chappé, N. André, D. Figarella-Branger. Evidence for new targets and synergistic effect of metronomic celecoxib/fluvastatin combination in pilocytic astrocytoma. *Acta Neuropathol. Commun.*, 2013, 1:17.

20 D. T. Manallack, R. J. Prankerd, E. Yuriev, T. I. Oprea, D. K. Chalmers. The Significance of Acid/Base Properties in Drug Discovery. *Chem. Soc. Rev.*, 2013, 42, 485-496.

21 M. P. Gleeson. Generation of a set of simple, interpretable ADMET rules of thumb. *J. Med. Chem.*, 2008, 51, 817-834.

22 M. J. Waring. Defining optimum lipophilicity and molecular weight ranges for drug candidates–Molecular weight dependent lower logD limits based on permeability. *Bioorg. Med. Chem. Lett.*, 2009, 19, 2844–2851.

23 H. Li, B. Lei, W. Xiang, W. Feng, Y. Liu, S. Qi. Differences in Protein Expression between the U251 and U87 Cell Lines. *Turkish Neurosurgery*, 2017, *27*, 894-903.

24 T. T. Wager, X. Hou, P. R. Verhoest, A. Villalobos. Moving beyond rules: the development of a central nervous system multiparameter optimization (CNS MPO)

approach to enable alignment of druglike properties. *ACS Chem. Neurosci.*, 2010, 1, 435-449.

25 F. Broccatelli, C. A. Larregieu, G. Cruciani, T. I. Oprea, L. Z. Benet. Improving the prediction of the brain disposition for orally administered drugs using BDDCS. *Adv. Drug Deliv. Rev.*, 2012, 64, 95-109.

26 R. Didziapetris, P. Japertas, A. Avdeef, A. J. Petrauskas. Classification analysis of P-glycoprotein substrate specificity. *Drug Target.*, 2003, 11, 391-406.

27 C. H. A. Lee, H. K. M. Nagaraj, A. D. William, M. Williams, Z. Xiong. Triazine compounds as kinase inhibitors. *WO* 2009/093981A1, 2009.

28 J. Waser, B. Gaspar, H. Nambu, E.-M. Carreira. Hydrazines and azides via the metal-catalyzed hydrohydrazination and hydroazidation of olefins. *J. Am. Chem. Soc.*, 2006, 128, 11693-11712.

29 L. J. Cotterill, R. W. Harrington, W. Clegg, M. J. Hall. Thermal 1,3-trityl migrations in Diels-Alder domino reactions of 1-trityl-4-vinyl-1H-imidazoles. *J. Org. Chem.*, 2010, 75, 4604-4607.

Chemical modifications of imidazole-containing alkoxyamines increase C–ON bond homolysis rate: effects on their cytotoxic properties in glioblastoma cells

Toshihide Yamasaki [a, #], Duje Buric [b, #], Christine Chacon [b], Gérard Audran [a], Diane Braguer [c,d], Sylvain R. A. Marque [a, e], Manon Carré [b, *], Paul Brémond [a,b, *]

Graphical Abstract: